fermentation

MDPI

Article

Conversion of Syngas from Entrained Flow Gasification of Biogenic Residues with *Clostridium carboxidivorans* and *Clostridium autoethanogenum*

Anton Rückel [1], Anne Oppelt [1], Philipp Leuter [2], Philipp Johne [2], Sebastian Fendt [2] and Dirk Weuster-Botz [1,*]

[1] Technical University of Munich, TUM School of Engineering and Design, Chair of Biochemical Engineering, 85748 Garching, Germany
[2] Technical University of Munich, TUM School of Engineering and Design, Chair of Energy Systems, 85748 Garching, Germany
* Correspondence: dirk.weuster-botz@tum.de; Tel.: +49-89-289-15712

Abstract: Synthesis gas fermentation is a microbial process, which uses anaerobic bacteria to convert CO-rich gases to organic acids and alcohols and thus presents a promising technology for the sustainable production of fuels and platform chemicals from renewable sources. *Clostridium carboxidivorans* and *Clostridium autoethanogenum* are two acetogenic bacteria, which have shown their high potential for these processes by their high tolerance toward CO and in the production of industrially relevant products such as ethanol, 1-butanol, 1-hexanol, and 2,3-butanediol. A promising approach is the coupling of gasification of biogenic residues with a syngas fermentation process. This study investigated batch processes with *C. carboxidivorans* and *C. autoethanogenum* in fully controlled stirred-tank bioreactors and continuous gassing with biogenic syngas produced by an autothermal entrained flow gasifier on a pilot scale >1200 °C. They were then compared to the results of artificial gas mixtures of pure gases. Because the biogenic syngas contained 2459 ppm O_2 from the bottling process after gasification of torrefied wood and subsequent syngas cleaning for reducing CH_4, NH_3, H_2S, NO_X, and HCN concentrations, the oxygen in the syngas was reduced to 259 ppm O_2 with a Pd catalyst before entering the bioreactor. The batch process performance of *C. carboxidivorans* in a stirred-tank bioreactor with continuous gassing of purified biogenic syngas was identical to an artificial syngas mixture of the pure gases CO, CO_2, H_2, and N_2 within the estimation error. The alcohol production by *C. autoethanogenum* was even improved with the purified biogenic syngas compared to reference batch processes with the corresponding artificial syngas mixture. Both acetogens have proven their potential for successful fermentation processes with biogenic syngas, but full carbon conversion to ethanol is challenging with the investigated biogenic syngas.

Keywords: *Clostridium carboxidivorans*; *Clostridium autoethanogenum*; syngas fermentation; real synthesis gas; syngas from gasification of biomass; autotrophic alcohol production; carbon monoxide conversion; oxygen inhibition; catalytic oxygen reduction

Citation: Rückel, A.; Oppelt, A.; Leuter, P.; Johne, P.; Fendt, S.; Weuster-Botz, D. Conversion of Syngas from Entrained Flow Gasification of Biogenic Residues with *Clostridium carboxidivorans* and *Clostridium autoethanogenum*. *Fermentation* **2022**, *8*, 465. https://doi.org/10.3390/fermentation8090465

Academic Editors: Zhiqiang Wen and Naief H. Al Makishah

Received: 31 July 2022
Accepted: 14 September 2022
Published: 17 September 2022

1. Introduction

Synthesis gas fermentation has emerged as a promising approach for the production of alcohols for fuels or platform chemicals from waste gases or renewable resources. The syngas fermentation process uses gas mixtures, which mainly consist of CO, CO_2, H_2, and N_2. These gases can be derived from various sources including industrial off-gas streams such as steel-mill off-gases or from gasification of carbon-rich material such as biomass. In addition to these main components, a syngas can contain various types of trace components, such as CH_4, O_2, HCN, NH_3, NO_X, H_2S, COS, and CS_2 [1–7]. The detailed composition can vary, depending on the composition of the used material for gasification and the applied gasification conditions, such as oxygen ratio or residence time [1,2,8–10].

The coupling of the gasification of biogenic residues, such as leaves, green cuttings, and wood shavings, with the fermentation of the biogenic syngas may be considered as an ecologically beneficial process by which to produce industrially relevant alcohols for usage as biofuels [11,12] or platform chemicals [13].

Acetogenic microorganisms can be utilized for the conversion of syngas under strictly anaerobic conditions by using the reductive acetyl-CoA pathway [14,15]. A number of microorganisms have shown a large potential for their utilization in syngas fermentation processes in recent years. Two of these microorganisms are *Clostridium carboxidivorans* and *Clostridium autoethanogenum*, due to their high tolerance toward high CO content in the syngas and for their potential of producing the industrially relevant alcohols ethanol, 1-butanol, and 1-hexanol [16–19], or ethanol, and 2,3-butanediol [20–22], respectively, with relatively low acetic acid production [16,23]. The optimum for growth of these microorganisms is between pH 5.8 and pH 6.0 at 37 °C [17,20,24]. The genomes of both microorganisms have already been completely sequenced and published [25–27]. *C. carboxidivorans* is most well-known for its ability to increase the chain length by adding acetyl-CoA to form butyrate and hexanoate. It is also known for its ability to reuptake already produced acids and the conversion of these into the corresponding alcohols 1-butanol, and 1-hexanol [16,28]. The formation of products by *C. carboxidivorans* is closely connected to the pH, having higher growth rates and acid production at high pH (pH 6) and alcohol production at lower pH (pH 5 and lower) [16,29,30]. Therefore, an initial pH 6.0 without pH control in the process leads to an initial phase with organic acid production, the so-called acidogenesis, and by the natural decrease of pH, a phase with alcohol production, the so-called solventogenesis [16,31]. An uncontrolled pH with the natural decrease of the pH by acid production and the following conversion to alcohol has been shown to give the best alcohol production in batch processes with *C. carboxidivorans* [16]. *C. autoethanogenum,* on the other hand, is known for its potential as an ethanol-producing microorganism and has already been made genetically accessible to increase alcohol production and to form non-natural products such as 2-propanol, and acetone [13,32,33]. The following chemical equations show the product formation reactions with their respective Gibbs' free energies [28,34].

$4CO + 2H_2O \rightarrow CH_3COOH + 2CO_2$	$\Delta G^0 = -154.6$ kJ mol^{-1}
$6CO + 3H_2O \rightarrow CH_3CH_2OH + 4CO_2$	$\Delta G^0 = -217.4$ kJ mol^{-1}
$10CO + 4H_2O \rightarrow CH_3(CH_2)_2COOH + 6CO_2$	$\Delta G^0 = -420.8$ kJ mol^{-1}
$12CO + 5H_2O \rightarrow CH_3(CH_2)_3OH + 8CO_2$	$\Delta G^0 = -486.4$ kJ mol^{-1}
$16CO + 6H_2O \rightarrow CH_3(CH_2)_4COOH + 10CO_2$	$\Delta G^0 = -656.0$ kJ mol^{-1}
$18CO + 7H_2O \rightarrow CH_3(CH_2)_5OH + 12CO_2$	$\Delta G^0 = -753.0$ kJ mol^{-1}
$11CO + 5H_2O \rightarrow C_4H_8(OH)_2 + 7CO_2$	$\Delta G^0 = -361.8$ kJ mol^{-1}
$2CO_2 + 4H_2 \rightarrow CH_3COOH + 2H_2O$	$\Delta G^0 = -74.3$ kJ mol^{-1}
$2CO_2 + 6H_2 \rightarrow CH_3CH_2OH + 3H_2O$	$\Delta G^0 = -97.0$ kJ mol^{-1}
$4CO_2 + 10H_2 \rightarrow CH_3(CH_2)_2COOH + 6H_2O$	$\Delta G^0 = -220.2$ kJ mol^{-1}
$4CO_2 + 12H_2 \rightarrow CH_3(CH_2)_3OH + 7H_2O$	$\Delta G^0 = -245.6$ kJ mol^{-1}
$6CO_2 + 16H_2 \rightarrow CH_3(CH_2)_4COOH + 10H_2O$	$\Delta G^0 = -341.0$ kJ mol^{-1}
$6CO_2 + 18H_2 \rightarrow CH_3(CH_2)_5OH + 11H_2O$	$\Delta G^0 = -395.0$ kJ mol^{-1}
$4CO_2 + 11H_2 \rightarrow C_4H_8(OH)_2 + 6H_2O$	$\Delta G^0 = -140.7$ kJ mol^{-1}
$2CO + 2H_2 \rightarrow CH_3COOH$	$\Delta G^0 = -114.5$ kJ mol^{-1}
$2CO + 4H_2 \rightarrow CH_3CH_2OH + H_2O$	$\Delta G^0 = -137.1$ kJ mol^{-1}
$4CO + 6H_2 \rightarrow CH_3(CH_2)_2COOH + 2H_2O$	$\Delta G^0 = -317.0$ kJ mol^{-1}
$4CO + 8H_2 \rightarrow CH_3(CH_2)_3OH + 3H_2O$	$\Delta G^0 = -334.0$ kJ mol^{-1}
$6CO + 10H_2 \rightarrow CH_3(CH_2)_4COOH + 4H_2O$	$\Delta G^0 = -540.0$ kJ mol^{-1}
$6CO + 12H_2 \rightarrow CH_3(CH_2)_5OH + 5H_2O$	$\Delta G^0 = -514.0$ kJ mol^{-1}
$4CO + 7H_2 \rightarrow C_4H_8(OH)_2 + 2H_2O$	$\Delta G^0 = -221.1$ kJ mol^{-1}

A variety of inhibiting components in syngases can affect the syngas fermentation process and are discussed in detail in review articles [3,5,7,18,21,35,36]. NH_3 is an inhibitor for hydrogenases in *C. ragsdalei* [3]. H_2S is known to inhibit the ascorbate oxidase in *Acremonium* sp., rhodanases, and thiosulfate sulfur transferases [37,38]. NO has been shown to inhibit hydrogenases in *C. carboxidivorans* at concentrations above 40 ppm NO

in a syngas [3,35]. NO_2 inhibits the formate dehydrogenase in *Pichia pastoris* and nitrate reductase in *Bradyrhizobium japonicum* [39,40]. Nitrate may serve as an alternative electron acceptor for acetogenic *Clostridia* like *C. ljungdahlii* [41] and has been shown to inhibit CO consumption of *C. carboxidivorans* [18]. Nitrite is toxic for most bacteria but can be used as an electron acceptor by some *Clostridia* like *M. thermoacetica* [42,43]. However, even low amounts of 0.1 g L^{-1} $NaNO_2$ were toxic for *C. carboxidivorans* [18]. One of the most critical impurities in biogenic syngases is HCN, which has been shown to have inhibiting and toxic effects on *C. ljungdahlii* above 0.027 g L^{-1} KCN [44]. Other less prominent impurities in biogenic syngases like COS are noncompetitive inhibitors for the CO dehydrogenase in *Rhodospirillum rubrum* [45].

Until now, the influence of oxygen as a trace component in syngas fermentation has rarely been studied in detail. Oxygen is a crucial component for the metabolism of strictly anaerobic microorganisms because O_2 serves as a strong oxidizing agent. The limit for anaerobic growth and product formation is closely connected to the enzyme with the highest critical redox potential, the methylene-THF/methyl-THF redox couple, which is reported to be in the range between −120 mV and −200 mV depending on the source [14,46–48]. Thus, an increased redox potential by oxygen in the syngas can affect the metabolism of anaerobic microorganisms [14,46,49]. Karnholz et al. [50] investigated the influence of oxygen on acetogenic bacteria, such as *C. magnum* and *A. woodii,* in anaerobic tubes and found considerable differences in the tolerances of different anaerobic microorganisms. However, in these studies the oxygen was not supplied continuously, as is the case with syngas fermentation processes in stirred-tank bioreactors. Kundiyana et al. [51] found almost no observable inhibition of *C. ljungdahlii* by oxygen levels in their reactor head space between 400 ppm and 26,000 ppm O_2 in a batch process in a pilot-scale stirred-tank reactor. In this study, the oxygen was not a part of the syngas stream, but rather came from an unidentified leakage in the reactor and was not constant throughout the process [51].

This study presents comprehensive data on batch processes by using the two acetogenic microorganisms *C. carboxidivorans* and *C. autoethanogenum* in continuously gassed stirred-tank bioreactors on a 1-L scale. Process performances of these two microorganisms were investigated with a biogenic and pre-purified syngas from the gasification of torrefied wood and an artificial syngas mixture of pure gases under identical process conditions to allow for a direct comparison. The initially high oxygen content in the biogenic syngas was reduced with a Pd catalyst in a tube reactor before entering the bioreactors to achieve an oxygen reduction in the syngas. The results were then compared to other results with these two microorganisms by using artificial syngas and defined gas impurities. Other studies have mainly investigated the conversion of biogenic syngas by using another acetogenic microorganism, *C. ljungdahlii* [4,6]. Despite its close genetic relation to *C. autoethanogenum* [52], *C. ljungdahlii* has shown a lower production of ethanol and higher accumulation of acetate than *C. autoethanogenum* [4,6,21]. *C. carboxidivorans,* on the other hand, has shown the highest tolerance toward common syngas impurities and is of high interest because of its unique product spectrum [18]. Therefore, the effects of biogenic syngas on these two microorganisms are of high interest for industrial applications [13,53]. This study also presents an outlook on optimal syngas compositions to achieve high syngas conversions by these microorganisms in industrial-scale bioprocesses applying bubble column or gas lift reactors.

2. Materials and Methods

2.1. Microorganisms, Media, and Preculture Conditions

The microorganisms utilized were obtained from the German Collection of Microorganisms and Cell Cultures (DSMZ, Braunschweig, Germany) as freeze-dried cultures of *C. carboxidivorans* P7 (DSM 15243), and *C. autoethanogenum* JA1-1 (DSM 10061). The cultivation medium was previously published by Doll et al. (2018) [16], and the detailed composition can be found in the supplementary material (Table S1).

The preculture medium was supplied with 15 g L^{-1} MES as a pH buffer and adjusted to pH 6.1 with NaOH. The medium was prepared anaerobically by boiling 2 L of the medium in a round flask for 20 min and subsequently flushing with N_2 for 20 min under cooling in an ice water bath. The medium was later aliquoted in portions of 100 mL into anaerobic bottles with 250 mL maximum volume under reducing atmosphere in an anaerobic glove-box with a gas mixture of 5% H_2, and 95% N_2. The bottles were then closed with a butyl-rubber septum and autoclaved for 20 min at 121 °C in a steam sterilization autoclave.

For pre-cultures of *C. carboxidivorans*, every anaerobic bottle was supplied with 5 g L^{-1} glucose by a sterile syringe and needle through the rubber septum. Afterward, 2.5 mL of a cryo-conserved culture were inoculated with approximately 0.05 g L^{-1} cell dry weight (CDW) by a sterile syringe and needle through the rubber septum, resulting in a final volume of 104.5 mL in the bottle. The anaerobic shaken bottles were then incubated at 37 °C and 100 min^{-1} for 22 h in a shaking incubator (WIS-20, Witeg, Wertheim, Germany).

For pre-culture preparations of *C. autoethanogenum*, anaerobic bottles for a first pre-culture were supplied with 5 g L^{-1} xylose by a sterile syringe and needle through the rubber septum. A total of 5 mL of a cryo-conserved culture were inoculated with approximately 0.05 g L^{-1} CDW by a sterile syringe and needle through the rubber septum resulting in a final volume of 107 mL in the bottle. The anaerobic shaken bottles were then incubated at 37 °C and 100 min^{-1} for 60 h in an incubator (WIS-20, Witeg, Wertheim, Germany). In a second pre-culture step, 10 mL of the first pre-culture was transferred to a new anaerobic bottle with 100 mL liquid medium, which was supplied with 10 g L^{-1} xylose and 0.4 g L^{-1} cysteine hydrochloride, by a sterile syringe and needle through the butyl rubber septum, resulting in a final volume of 115 mL in the bottle. These bottles were then incubated at 37 °C and 100 min^{-1} for 22 h in an incubator (WIS-20, Witeg, Wertheim, Germany).

Both microorganisms were harvested by anaerobically transferring the pre-cultures into centrifugal tubes and centrifuging them at 3260 RCF for 10 min at room temperature. The tubes were then transferred into the anaerobic glove-box (5% H_2 and 95% N_2), and the supernatant was discarded. The pellet was resuspended in 10 mL anaerobic phosphate-buffered saline (12 mM phosphate) and was then inoculated to the stirred-tank bioreactor to achieve an initial cell dry weight concentration of 0.05 g L^{-1} CDW.

2.2. Conditions for Batch Processes in Stirred-Tank Bioreactors

All processes presented in this study were batch processes in a continuously gassed, stainless steel, stirred-tank bioreactor (KLF2000, BioEngineering, Wald, Switzerland) with a working volume of 1 L. The bioreactor was supplied with two radially mixing six-blade stirrers (Rushton turbines), a sampling valve at the bottom, two side entries for a pH- and a redox-probe, and a lid with a safety valve, the syngas inlet, two inlets for acid and base, and the exhaust-gas line with a cooler, a sterile filter, and a pressure control valve. The probes for pH and redox measurements were calibrated before sterilization between pH 4.0–pH 7.0, and 220–468 mV at 37 °C, respectively. The reactor off-gas was cooled to 2 °C to avoid loss of liquid volume by evaporation of water as well as loss of volatile products like alcohols. 3 M NaOH, and 1 M H_2SO_4 were used for pH correction. pH was controlled at pH 6.0 for processes with *C. autoethanogenum*, whereas the initial pH 6.0 was not controlled in processes with *C. carboxidivorans*.

The reactor was sterilized *in situ* with 1 L of demineralized water and heated to 121 °C at 2.2 bar for 20 min. Afterward, the pressure was slowly released from the reactor to 1.2 bar during cooling. After cooling down to 65 °C, the water was released through the sampling valve at the bottom of the reactor. A total of 1 L of medium was prepared without vitamins, cysteine, MES, or sugar and autoclaved in a coated 1-L glass bottle with a butyl rubber septum for 20 min at 121 °C. The medium was transferred through a sterile needle and a sterilized silicone tube to the reactor. After the medium had cooled down to 37 °C, 10 mL of the vitamin solution was added sterile to the medium through a syringe filter with 0.2 µm pore size. The medium was anaerobized in the reactor by purging with

N_2 at 5 NL h^{-1} for 2 h and afterward with the desired gas mixture or biogenic syngas at 5 NL h^{-1} for at least 12 h. A gas supply of artificial syngas mixtures was applied by using a gas mixing system with four thermal mass flow controllers (P-702CV-6K0R-RAD-33-V, Bronkhorst, Reinach, Switzerland). A gas supply of syngas from gasification of biomass was achieved with a mass flow controller for corrosive gases (F-201CV-500-RGD-33-V, Bronkhorst, Reinach, Switzerland). A total of 10 mL of 40 g L^{-1} cysteine hydrochloride solution was added to the reactor immediately before inoculation as a reducing agent. The volumetric power input by the stirrer was constant at 15.1 W L^{-1}, and the temperature was constant at 37 °C in all presented batch processes.

2.3. Syngas Production and Purification

2.3.1. Biomass Gasification-BOOSTER Test Rig

The biomass pilot-scale entrained flow gasifier (BOOSTER) [1,2] is an autothermal refractory lined entrained flow gasifier with a thermal biomass input power at the operating point for the syngas production of 120 kW. In steady-state operation, wall temperatures of 1450 °C are reached in the flame region of the reaction chamber, while temperatures cool down to around 1150 °C at the end of the reactor. Pure oxygen preheated to 300 °C with an oxygen ratio of $\lambda = 0.5$ is used as gasification agent. A steam ratio of $\varphi = 0.4$ kg_{steam} $kg_{fuel}{}^{-1}$ is used as moderator. The biogenic pulverized fuel, torrefied wood (TorrCoal) with a particle size < 250 µm, is fed into the reactor via a pneumatic dense phase conveying system with nitrogen as a dosing medium. The fuel composition is the following (as received): 57.3 wt% C, 5.0 wt% H, 0.3 wt% N, 30.9 wt% O, 1.5 wt% ash, and 5.0 wt% moisture. Particle residence times are estimated at 120 kW thermal input to around 2–3 s. The substoichiometric reaction produces a synthesis gas mixture consisting of the components CO, H_2, CO_2, and CH_4 as well as particles, tars, and trace gas impurities. This gas mixture is quenched to 50 °C with injected water at the end of the reaction zone. More information about the test rig is found in [1,2].

2.3.2. Syngas Cleaning Test Rig

A partial flow $\dot{V}_{syngas} = 9.8 \pm 3.1$ L min^{-1} of the produced syngas after the quench is fed into the downstream syngas cleaning test rig. The remaining syngas stream is sent to the flare. The following cleaning stages were applied: particle impurities > 2 µm separated with a heated ceramic cartridge filter. Water-soluble trace gas impurities and particles < 2 µm were removed in a countercurrent packed absorption column with water as a solvent ($\dot{V}_{solvent} = 3.0 \pm 0.03$ L min^{-1} at $T_{solvent} = 5.8 \pm 0.1$ °C). In addition, 3.8% CO_2 is scrubbed by the water from the total syngas stream. Afterward, the gas stream is cooled to 4.2 ± 0.6 °C in a glycol-cooled heat exchanger, and the water contained in the gas condenses. The final adsorptive purification step consists of four heated fixed-bed adsorption columns. Adsorption column 1 is operated at 45.2 ± 0.8 °C with activated carbon to separate hydrocarbons. For adsorption column 2, the adsorbent Al_2O_3 is applied at a temperature of 159.0 ± 5.0 °C to remove halogens. Adsorption column 3 runs at 151.1 ± 4.8 °C with ZnO for the removal of sulfur components. Adsorption column 4 is operated at 43.2 ± 0.9 °C with a catalytic activated carbon for the reduction of nitrogen oxides and as a "police filter". The gas hourly space velocity (GHSV) at the operating point in all adsorption columns is GHSV = 3614 ± 1106 h^{-1}.

The purified syngas is buffered in a nitrile-coated gas bag and filled into standard T50 tanks by using an electrically driven and dry-running syngas compressor (HAUG.Neptune 33G, HAUG Sauer Kompressoren AG, St. Gallen, Switzerland). A syngas composition of CO = 34.1%, H_2 = 22.7%, CO_2 = 13.8% is achieved at the operating gasification point used. The additional nitrogen input due to dosing and purge gases (e.g., flame camera) is N_2 = 10.6%. During this filling process, additional nitrogen N_2 = 18.5% and oxygen O_2 = 0.3% are entering the syngas by purging processes and safety valves.

2.3.3. Catalytic Oxygen Reduction in a Tube Reactor

Additionally, for processes with reduction of oxygen from the syngas, a tube reactor was filled with 30 g Pd-catalyst (Actisorb O3, 3–5 mm diameter, Clariant, Muttenz, Switzerland) and 10 g silica gel beads (silica gel orange, 2–5 mm diameter, Carl Roth, Karlsruhe, Germany). The metal catalyst allows for the reduction of the oxygen in the syngas with the hydrogen to form water. The water is then adsorbed into the silica gel beads to avoid condensation in the tube reactor or at the hydrophobic surface of the gas inlet sterile filter of the bioreactor. The tube reactor was made entirely of commercially available standard parts—a tube of 1.4571 stainless steel with a length of 1 m and an inner diameter of 10 mm, cutting ring fittings made of 1.4571 stainless steel, and a sieve at the bottom of the tube made of 1.4401 stainless steel (all stainless steel parts, Landefeld, Kassel, Germany). The stainless steel tube reactor was equipped with polyurethane tubing at the inlet and outlet to allow a modular connection to the gas supply system of the stirred-tank bioreactor. The tube reactor was heated by a water-filled silicone tube heating coil with a thermostat (Julabo, Seelbach, Germany), which was used to heat the gas stream to temperatures of 25 °C, 40 °C, or 50 °C, respectively. Temperatures higher than 50 °C were not applied to avoid an increase of possible side reactions such as the formation of methane. The oxygen content of the syngas after the tube reactor is shown in Figure 1 as a function of mean hydraulic residence time at varying temperatures. The mean hydraulic residence time in the tube reactor was 56.5 s to achieve the desired gas flow rate of 5.0 NL h^{-1} in the stirred-tank bioreactor. A temperature of 50 °C was chosen for syngas fermentation processes to reduce the oxygen content in the syngas from 2459 ppm to 293 ppm O_2.

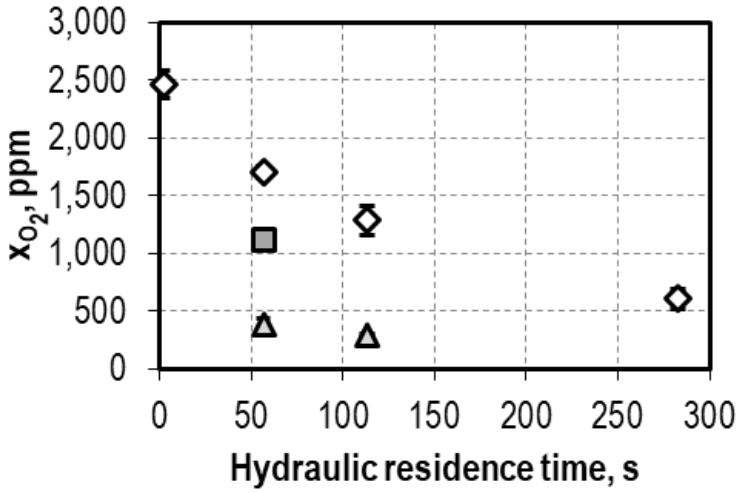

Figure 1. Oxygen reduction from a biogenic syngas from entrained flow gasification of biogenic residues (torrefied wood, TorrCoal) by a plug flow reactor (inner diameter 10 mm; length 1000 mm) filled with 30 g Pd-catalyst particles and 10 g silica beads at temperatures of 25 °C (white diamonds), 40 °C (dark grey square), and 50 °C (light grey triangle) as a function of the mean hydraulic residence time in the plug flow reactor. p_{CO} = 300 mbar, p_{H2} = 220 mbar, p_{CO2} = 90 mbar, p_{N2} = 390 mbar. Error bars indicate the standard deviation of a minimum of 10 measurements per data point.

2.4. Analytical Methods

2.4.1. Liquid Product Analysis

Liquid samples were collected through an outlet valve at the bottom of the bioreactor and were measured for optical density at 600 nm (OD_{600}) in a spectrophotometer (Genesys 10S UV–Vis, Thermo Scientific, Neuss, Germany). Samples with optical densities higher than OD_{600} 0.3 were diluted with PBS to achieve an OD_{600} between 0.1 and 0.3. All samples for optical density measurements were measured in triplicates. The optical densities were then used to estimate cell dry weight concentrations by the previously determined linear

correlation factors of 0.46 g L^{-1} OD^{-1} for *C. carboxidivorans*, and 0.38 g L^{-1} OD^{-1} for *C. autoethanogenum*, respectively [16,18,21].

Products were measured with an HPLC instrument (LC-2030C, Shimadzu, Kyoto, Japan), which was equipped with a refractive index detector (RID-20A, Shimadzu, Kyoto, Japan) and a cation exchange separation column (Aminex HPX-87H, Bio-Rad, Munich, Germany). Elution conditions were isocratic 5 mM H_2SO_4 with a flow rate of 0.6 mL min^{-1} and a column temperature of 60 °C. All measurements carried an individual standard series of at least five different concentrations of the target components. The concentrations of the dilution series were between 0.1 g L^{-1} and 5.0 g L^{-1} for formic acid, ethanol, 1-butanol, butyric acid, hexanoic acid, and 2,3-butanediol. The concentrations of the standard series were between 0.2 g L^{-1} and 10.0 g L^{-1} for glucose, xylose, and acetic acid. All samples with 1-hexanol were concentrated before the measurement by extraction with ethyl acetate. A standard series of 1-hexanol with concentrations from 0.08 g L^{-1} to 2.0 g L^{-1} was prepared and likewise extracted. Therefore, 300 µL ethyl acetate was added to 900 µL of the sample in a safe-lock vessel and shaken in a shaking mill (MM200, Retsch, Haan, Germany) at 25 s^{-1} for 15 min. The vessels were then centrifuged in a bench-top centrifuge at 13,000 min^{-1} for 3 min to improve phase separation, and 125 µL of the organic phase was transferred to a glass vial for HPLC measurement. The measurement was then conducted identically to the other samples.

2.4.2. Synthesis Gas Analysis

Exhaust gas was analyzed with a combination of mass flow measurement and gas composition measurement. Mass flow was analyzed with a thermal mass flow meter (F-101D-RAD-33-V, Bronkhorst, Reinach, Switzerland) for artificial syngas mixtures and with a special mass flow meter for corrosive gas (F-111B-500-RGD-33-V, Bronkhorst, Reinach, Switzerland) for the biogenic syngas. Micro-gas chromatography (micro GC 450, Agilent Technologies, Waldbronn, Germany) measurements were applied to measure the concentrations of the main syngas components CO, CO_2, H_2, and N_2 and of the trace components O_2, CH_4 NH_3, H_2S, HCN, and NO_X. The µGC was supplied with three channels for simultaneous measurement of the different syngas components in three individual thermal conductivity detectors (TCD) and three individual separation columns (Channel 1: molecular sieve, carrier gas argon, 80 °C, 250 kPa, for the separation of H_2, O_2, N_2, CH_4, and CO; Channel 2: PlotPQ, carrier gas helium, 80 °C, 150 kPa, for the separation of CO_2, NH_3, HCN, and NO_X; Channel 3: CP-Sil 5, carrier gas helium, 45 °C, 100 kPa, for the separation of CO_2, and H_2S). Gas consumption and production rates for the main syngas components CO, CO_2, and H_2 were estimated by multiplying the individual gas partial pressure measured by µGC with the exhaust gas flow rate measured by the mass flow meter. The total consumption of each gas component was measured by numerically integrating the gas uptake rate with a time step of 10 min.

3. Results

3.1. Batch Process Performances of C. carboxidivorans with Artificial and Biogenic Syngas

Batch processes with *C. carboxidivorans* were conducted with an artificial syngas mixture and a syngas from the gasification of biogenic residues (TorrCoal). The original syngas was used directly for two batch processes and was additionally used for two batch processes with oxygen reduction in the tube reactor with Pd catalyst (Actisorb O3). The detailed composition of the artificial syngas and the biogenic syngases with or without oxygen reduction is given in Table 1. The results with *C. carboxidivorans* of three independent reference batch processes are depicted in Figure 2 compared to the processes with biogenic syngas.

Table 1. Composition of artificial syngas and real syngas from entrained flow gasification of biogenic residues (torrefied wood, TorrCoal) without reduction of oxygen, and with reduction of oxygen by a plug flow reactor (inner diameter 10 mm; length 1000 mm) with 30 g Actisorb O3 and 10 g silica beads at a temperature of 50 °C.

Syngas Component	Artificial Syngas	Biogenic Syngas after Syngas Cleaning	Biogenic Syngas after Syngas Cleaning with Additional Oxygen Reduction
N_2	36.7 ± 0.3%	34.4 ± 2.9%	30.2 ± 3.8%
CO	30.1 ± 0.4%	30.3 ± 1.7%	31.6 ± 3.4%
CO_2	10.3 ± 0.2%	9.4 ± 0.7%	10.0 ± 1.1%
H_2	18.5 ± 0.1%	22.2 ± 0.4%	21.9 ± 1.7%
CH_4	<<0.1%	0.46 ± 0.009%	0.51 ± 0.034%
O_2	<<50 ppm	2459 ± 122 ppm	293 ± 5 ppm
NH_3	<1 ppm	3099 ± 181 ppm	766 ± 344 ppm
H_2S	<1 ppm	<50 ppm	<50 ppm
NO_X	<1 ppm	<1 ppm	<1 ppm
HCN	<1 ppm	<1 ppm	<1 ppm

The processes with *C. carboxidivorans* using biogenic syngas without oxygen reduction led to drastically reduced growth and product formation with no observable alcohol production in the entire process time (Figure 2) and also no gas uptake of CO or CO_2 (see supplementary material Figure S2). The redox potential steadily increased by the oxygen content in the syngas and reached critical levels of −200 mV (see supplementary material Figure S1). In the following batch process, the redox potential was controlled by the addition of 2 g L^{-1} cysteine hydrochloride after 32 h and 78 h (see supplementary material Figure S1). However, even after keeping the redox potential below −250 mV, the growth and the production of alcohols stayed low. A total amount of 2 g L^{-1} cysteine hydrochloride was necessary to keep the redox potential below −250 mV throughout the entire process.

In additional batch processes, the biogenic syngas was led through a tube reactor with a Pd catalyst (Actisorb O3) to reduce the oxygen content of the syngas from 2459 ppm to 293 ppm O_2. The two batch processes performed with oxygen-reduced biogenic syngas show a higher deviation compared to the three reference batch processes. However, the average concentration of cell dry weight, acetate, and ethanol are in the same order of magnitude as the reference batch processes. The concentrations of 1-butanol, and 1-hexanol were slightly reduced with the biogenic syngas, but reached the same maximum concentrations. Despite the high reproducibility of the concentrations of cell dry weight, acetate, and ethanol, there was a high deviation of the measured 1-hexanol concentrations in the two processes with biogenic syngas, which could not yet be explained.

The carbon balance recovery for the reference batch process with *C. carboxidivorans* was 93.9 ± 0.4%. The processes with biogenic syngas from gasification of biomass with oxygen reduction resulted in carbon balance recoveries of 93.2% and 89.7%. Carbon balances are not fully closed, probably because of unconsumed carbon sources provided initially in the medium (yeast extract and cysteine) and the evaporation of alcohols. Further details on gas uptake rates, total gas consumption, and carbon balance recovery can be found in the supplementary material (Tables S2 and S3, Figures S1 and S2).

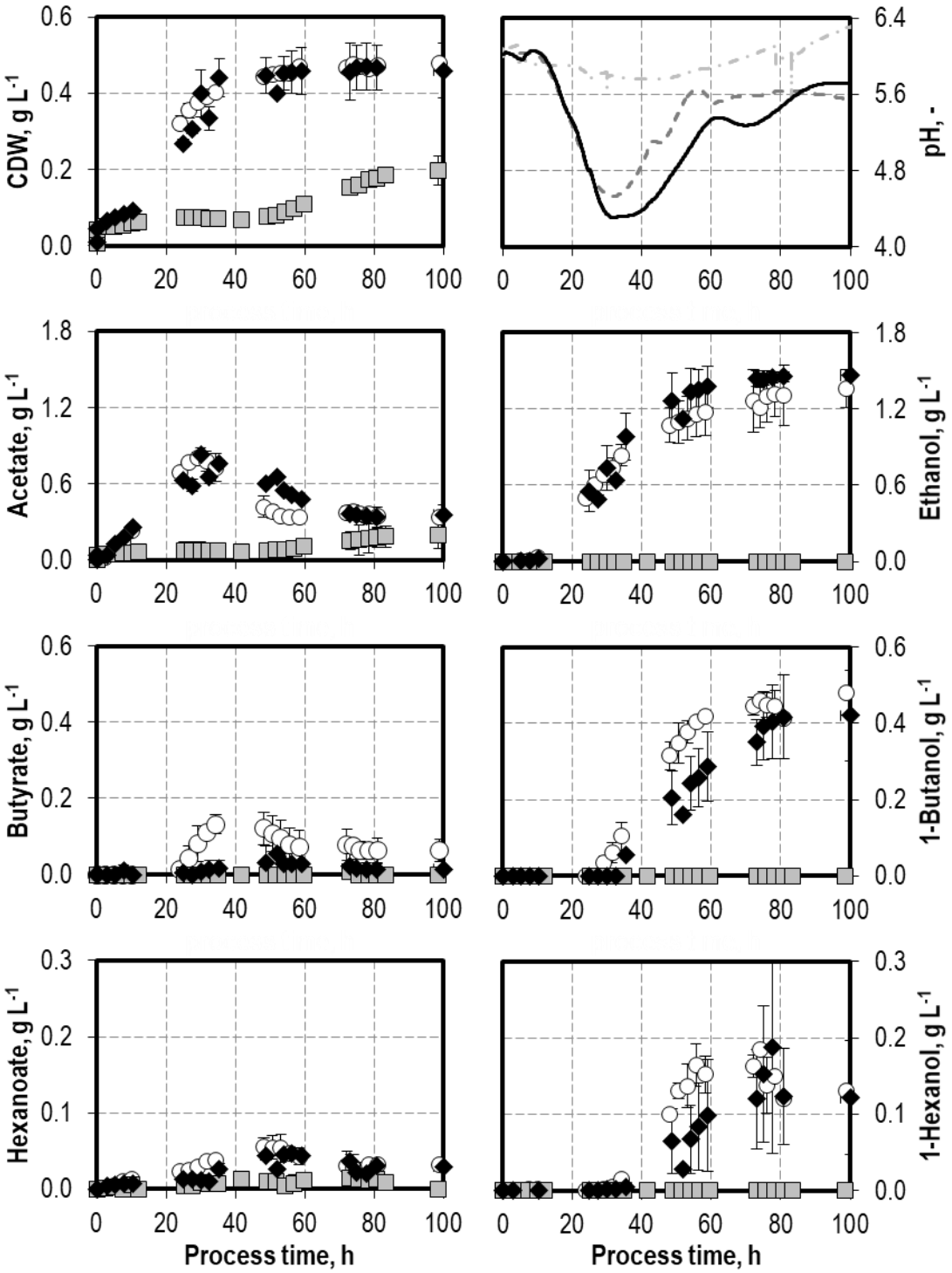

Figure 2. Autotrophic reference batch processes with *C. carboxidivorans* with artificial syngas (white circle, dark grey dashed line), batch processes with real syngas from entrained flow gasification of biogenic residues (torrefied wood, TorrCoal) (light grey square, light grey dash-dot line), and batch processes with biogenic syngas with oxygen reduction by a Pd catalyst (Actisorb O3) (black diamond, black solid line). Reaction conditions were constant at T = 37 °C, P V^{-1} = 15.1 W L^{-1}, F_{gas} = 5 NL h^{-1}, $pH_{initial}$ = 6.0 (uncontrolled unless > pH 6.4); p_{CO} = 300 mbar, p_{H2} = 220 mbar, p_{CO2} = 90 mbar, p_{N2} = 390 mbar. Error bars indicate standard deviations of three individual reference batch processes with artificial syngas, and the respective minimum and maximum values of two individual batch processes with the biogenic syngases. pH values depict the curve of one representative batch process.

3.2. Batch Process Performances of *C. autoethanogenum* with Artificial and Biogenic Syngas

The results of three individual reference batch processes with artificial syngas are compared to one batch process with biogenic syngas after oxygen reduction with Pd catalysts in the tube reactor (Figure 3). Reproduction of the batch process with biogenic syngas was not possible due to the total consumption of the biogenic syngas available from this gasification campaign.

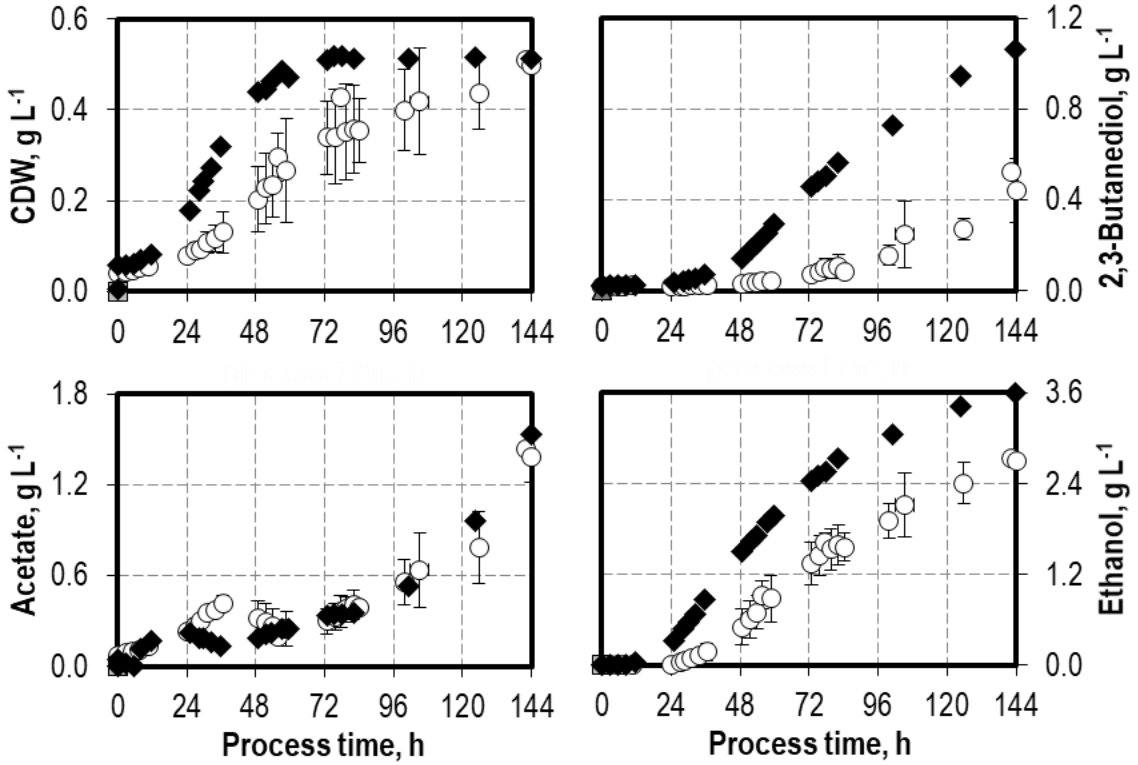

Figure 3. Autotrophic reference batch processes with *C. autoethanogenum* with artificial syngas (white circle), and batch processes with real syngas from entrained flow gasification of biogenic residues (torrefied wood, TorrCoal) after oxygen reduction by a Pd catalyst (Actisorb O3) (black diamond). Reaction conditions were constant at T = 37 °C, P V^{-1} = 15.1 W L^{-1}, F_{gas} = 5 NL h^{-1}, pH = 6.0 (controlled with 3 M NaOH and 1 M H_2SO_4); p_{CO} = 300 mbar, p_{H2} = 220 mbar, p_{CO2} = 90 mbar, p_{N2} = 390 mbar. Error bars indicate standard deviations of three individual reference batch processes with artificial syngas. The batch process with biogenic syngas was carried out once.

Despite the similar composition of the biogenic and the artificial syngas (Table 1), the batch process with biogenic syngas having a reduced oxygen concentration led to an increase in specific growth rate and the maximum concentrations of alcohols. The final ethanol concentration was increased by 31% from 2.74 g L^{-1} to 3.60 g L^{-1} and the final 2,3-butanediol concentration by 104% from 0.52 g L^{-1} to 1.06 g L^{-1} after six days. The maximum acetic acid and cell dry weight concentrations achieved with the biogenic syngas were not different from the three reference batch processes. The increased alcohol formation with the biogenic syngas is clearly beyond the standard deviation of the three independent reference batch processes.

The carbon balance recovery for the reference batch process with *C. autoethanogenum* was 89.4 ± 11.4% with a relatively high standard deviation. The carbon balance of one of the batch processes could only be closed partly due to unknown reasons (73.9%). The process with biogenic syngas from gasification of biomass with oxygen reduction resulted in a carbon balance recovery of 92.1%. Carbon balances are not fully closed, probably because of unconsumed carbon sources provided initially in the medium (yeast extract and cysteine) and the evaporation of alcohols. Further details on gas uptake rates, total gas

consumption, and carbon balance recovery can be found in the supplementary material (Table S4, Figures S1 and S4).

4. Discussion

4.1. Influence of Oxygen Impurities on Syngas Fermentation Processes with C. carboxidivorans

Oxygen as a strong oxidizing agent has an increasing effect on the redox potential. Despite its low water solubility of 22.98 µmol O_2 mol^{-1} at 25 °C and 1013 mbar [54], the oxygen input of a syngas with 2459 ppm was too high for anaerobic growth of *C. carboxidivorans*. The oxygen led to increasing redox potential, exceeding critical values for anaerobic metabolism of −200 mV [14,47,48]. However, the controlled reduction of the redox potential by addition of cysteine hydrochloride is economically unviable because of the high price of cysteine and the low added value of the syngas fermentation process [53,55]. The reduction of the oxygen content of the biogenic syngas with a Pd-catalyst to 293 ppm enabled biogenic syngas fermentation processes with both *C. carboxidivorans* and *C. autoethanogenum*, comparable to artificial syngas without oxygen. A more sophisticated statistical analysis of the obtained fermentation results is challenging because of the low number of reproductions for the processes with biogenic syngas, whereas the reference batch processes with synthetic syngas have been reproduced three times (see Figures 2 and 3). The biogenic syngas in this study was obtained in an entrained flow gasification campaign, which didn't provide sufficient amounts of syngas for another reproduction with identical syngas from the identical fuel (TorrCoal). Therefore, the processes with *C. autoethanogenum* with biogenic syngas in particular should be repeated with biogenic syngas from another longer-lasting gasification campaign in the future. However, the results in this study showed successful syngas fermentation processes with both microorganisms using the biogenic syngas.

4.2. Comparison to Other Syngas Fermentation Processes with Pure and Biogenic Syngas

Compared to batch processes with artificial syngas in earlier studies, slightly lower maximum cell dry weight, and ethanol concentrations were measured due to the lower CO content in the artificial syngas in this study. Batch processes in the same reactor system with a gas mixture of 800 mbar CO and 200 mbar CO_2 and with additions of ammonium and hydrogen sulfide have resulted in higher maximum alcohol concentrations of up to 3.2 g L^{-1} ethanol, 1.1 g L^{-1} 1-butanol, and 0.29 g L^{-1} 1-hexanol, respectively, with *C. carboxidivorans* [18]. *C. carboxidivorans* is known for its preference toward high CO contents with an optimum between 40% and 80% CO [7,16,19]. *C. autoethanogenum* has also shown higher final biomass and alcohol concentrations of 0.67 g L^{-1} cell dry weight, 4.45 g L^{-1} ethanol, and 1.94 g L^{-1} 2,3-butanediol, respectively, with syngas mixtures of 600 mbar CO, 200 mbar CO_2, and 200 mbar H_2 in a stirred-tank reactor with continuous gassing [21].

C. ljungdahlii has already been successfully applied for the conversion of biomass-derived syngas in batch processes [4,6]. The autotrophic conversion of a syngas from the gasification of beech wood (28.5% CO, 19.1% CO_2, 22.7% H_2, 9.9% CH_4) resulted in a higher production of acetic acid (15.6 g L^{-1}, factor 9.75) and lower production of ethanol (1.6 g L^{-1}, factor 2.25) compared to the results achieved with *C. autoethanogenum* in this study [6]. However, higher alcohol concentrations usually are beneficial because of their higher added value compared to organic acids and their application as fuels or fuel additives [11,53]. Furthermore, longer-chain alcohols and bifunctional alcohols have a generally higher added value because of their usability as solvents and platform chemicals. In particular, 2,3-butanediol is relevant for its possible usage as an educt for the production of 1,3-butadiene as an important comonomer for the production of duroplastics [56]. A high final alcohol-to-acid ratio is also an important aspect for downstream processing in the purification of the produced alcohols [53,57].

4.3. Challenges and Opportunities on High Syngas Conversion in Industrial Scale Bioreactors

A high conversion of the supplied biogenic syngas components CO, H_2, and CO_2 into the desired product is a crucial economic aspect of syngas fermentation processes.

However, most acetogenic microorganisms show a high preference to CO toward CO_2/H_2 as the gaseous substrate [7,16,21]. The more negative Gibbs' free energy of the reactions with CO makes them thermodynamically preferable compared to CO_2 and H_2 [28]. The generation of electrons from CO is particularly preferred compared to electron generation from H_2 under any circumstances [58]. Therefore, conversion of CO_2 and H_2 by acetogens is observed most often only when the concentration of dissolved CO decreases under a very low threshold value. As an example, simultaneous conversion of CO and CO_2/H_2 was observed at a CO partial pressure of 20 mbar with a syngas composition of 2% CO, 23% CO_2, and 65% H_2 with *C. autoethanogenum* in a continuously operated stirred-tank reactor at a dilution rate of 0.5 d^{-1} [59].

Syngas fermentation on an industrial scale is performed in bubble column or gas-lift reactors [53,60]. The utilization of bubble columns instead of stirred-tank reactors is important due to the lower power input and more efficient syngas conversion at high liquid heights [61]. In an industrial scale stirred-tank bioreactor, the power input by the stirrer to increase the gas–liquid mass transfer rates is typically the main expense factor of the operating costs. Because the market price of the main syngas fermentation product ethanol is still rather low, cost efficiency plays a major role in syngas fermentation processes. In a typical bubble column reactor with a liquid height of 30 m, the hydrostatic pressure of the water column allows for higher solubilities of the syngas components at the bottom [62]. Conversion of CO by the acetogens decreases the CO content in the rising gas bubbles over the height of the reactor, and thus, a well-designed bubble column reactor will enable high conversion of the CO in the lower part of the reactor followed by the conversion of CO_2 and H_2 in the upper part of the bubble column.

The stoichiometry for the sole autotrophic conversion of CO leads to the release of 1 mol CO_2 per 2 mol CO for acetate production and 1 mol CO_2 per 1.5 mol CO for ethanol production [28]. Therefore, the CO_2 content of the rising gas bubbles will increase in the bubble column reactor. To achieve high conversion of CO_2 and H_2, the ratio between these gas components has to be in the range of H_2:CO_2 of 2:1 (for acetate production) to 3:1 (for ethanol production) [14,28]. As a consequence, the ideal stoichiometric ratio of H_2:CO in the syngas for total conversion of both components in a bubble column or gas-lift bioreactor would be 2:1 for sole ethanol production, and 1:1 for sole acetate production.

A biogenic syngas with the composition in this study would result in a gas stream with 34.2% CO_2, 24.5% H_2, and 41.3% N_2 after the first part of the reactor assuming full conversion of CO and exclusive ethanol production. Under the assumption of total conversion of the H_2 and the sole production of ethanol in the second part of the reactor, a gas composition of 38.7% CO_2, and 61.3% N_2 would remain in the reactor off-gas. However, the total off-gas stream would decrease to 39.7% of the initial syngas stream. The biogenic syngas would need a higher H_2 to CO_2 ratio to ensure a high CO_2 conversion. As autotrophic CO conversion results in CO_2 release, an ideal syngas from gasification of biomass would have as little CO_2 as possible. The majority of N_2 and O_2 in the investigated syngas came from the bottling process by dosing amounts, purging processes, and safety valves. Therefore, a directly coupled industrial process would result in lower N_2 content and lower to almost no O_2 content in the biogenic syngas [1,2]. The high CO_2 concentration in the investigated syngas mainly results from the low product gas temperature at the end of the reactor (thermal losses and non-ideal quench geometry), the high O content and non-ideal particle size distribution of the biomass. An ideal entrained flow gasification process in the given gasification rig could achieve a CO_2 content of 5% CO_2 [1,2]. The N_2 in the given syngas could be reduced by direct coupling of the gasification plant to the bioreactor to avoid N_2 input by dosing and purging. However, a remaining content of 10% N_2 in the given gasification rig is a realistic limit [1,2]. With an optimally achievable CO_2 concentration of around 5% in an ideal biogenic syngas and with a reduced N_2 content compared to this study, a composition of 23.3% CO, 5.0% CO_2, 61.7% H_2, and 10.0% N_2 would theoretically enable full conversion of the syngas components CO, CO_2, and H_2 in an ideally operated bubble column reactor.

4.4. Optimizing the Composition of Syngases from Gasification of Biomass

An entrained flow gasification process should aim to reach a viable composition of the resulting syngas by keeping CO and H_2 content high and the CO_2 content low. The typical elemental composition of wood residues (TorrCoal) on a molar basis is 38.0% C, 44.6% H, and 17.0% O, 53.1% (*w*/*w*) C, 5.2% (*w*/*w*) H, and 31.7% (*w*/*w*) O) [1]. Therefore, the high optimal H_2:CO ratio of 2:1 cannot be achieved with classical entrained flow gasification. Possibilities to increase the H_2 content in a syngas can be the addition of steam to the gasification agent, but might not be sufficient to reach 2:1 [63]. Plasma entrained flow gasification with steam as gasification agent could possibly achieve the necessary H_2:CO ratio, but is still at a rather low technology readiness level [64–66]. Additionally, hydrogen addition to the syngas from other sources such as chloralkali electrolysis, polymer electrolyte membrane electrolysis (PEM) or a subsequent water–gas shift reactor could be applied to achieve the necessary H_2:CO ratio. The latter would result in a loss of CO_2. The desired high CO:CO_2 ratio on the other hand could be achieved, especially by increasing the reactor temperature and optimizing oxygen–fuel ratio, residence time, or addition of reforming catalysts [1,2,9,10,63,67]

4.5. Outlook on Future Syngas Fermentation Research

The novelties of this study are (i) the combination of entrained-flow gasification with subsequent purification of the biogenic syngas and syngas fermentations applying *C. carboxidivorans* as well as *C. autoethanogenum* at well-defined reaction conditions in fully controlled stirred-tank bioreactors; (ii) the effects of traces of oxygen in a biogenic syngas on syngas fermentation processes with *C. carboxidivorans*; and (iii) in the comparison of the process performances of two highly promising acetogens under comparable process conditions in an identical bioreactor system with an identical biogenic syngas. The results of this work may serve as a basis for the transfer of syngas fermentation processes to an industrial scale. The entrained-flow gasification system with subsequent gas purification provided a syngas, which could successfully be used as a substrate for syngas fermentation processes with *C. carboxidivorans* and *C. autoethanogenum*. The identified critical and acceptable concentrations of traces of oxygen in real syngas could serve as a basis for detailed identification of the oxygen threshold concentration. Future studies on biogenic syngas fermentation processes with the acetogens under study could make use of syngas with higher contents of the other syngas impurities to identify their threshold concentrations, especially in combination. The modular syngas purification rig applied in this study could abandon one or more of the four fixed-bed adsorption columns to leave certain impurities in the syngas. This would also support the industrial application of processes converting biogenic syngas, because an economic industrial scale syngas fermentation process may require gas purification cost savings due to the low added value of the fermentation products. The detailed gas composition of the biogenic syngas could be adjusted to allow for a better ratio of the individual gas components and, thus, a higher conversion of the syngas components. Additionally, future research could apply pilot scale bubble column bioreactors to mimic more closely the conditions in an industrially applied syngas fermentation process [61]. Syngas fermentation remains a promising technology for the production of fuels and platform chemicals from renewable sources by using acetogenic microorganisms. Lastly, future research could investigate recombinant strains of the acetogenic microorganism to either increase the robustness toward certain impurities, to increase the alcohol productivity of the microorganisms, or to produce other, nonnatural products.

5. Conclusions

The results of this study indicated that the autotrophic conversion of a biogenic syngas with *C. carboxidivorans* and *C. autoethanogenum* showed comparable process performances in batch processes with continuous gassing in stirred-tank bioreactors compared to reference batch processes with artificial syngas. It was further confirmed that oxygen can be a crucial trace component in syngas fermentation processes. A total of 2459 ppm O_2 was found to

be inhibiting the autotrophic growth of *C. carboxidivorans* and no alcohol formation was observed, even if cysteine was supplied as a reducing agent to the reactor. Reducing the oxygen content to 293 ppm in the biogenic syngas applying Pd catalysts enabled batch process performances as in the reference batch processes with *C. carboxidivorans*. Both acetogens under study have proven their potential for successful fermentation processes with biogenic syngas. Based on theoretical considerations, full carbon conversion to ethanol is challenging with biogenic syngas. An ideal syngas from gasification of biomass should have as little CO_2 as possible.

Supplementary Materials: The following supporting information can be downloaded at: https://www.mdpi.com/article/10.3390/fermentation8090465/s1; Table S1: Composition of the liquid cultivation medium previously described by Doll et. al. (2018) [16] for anaerobic pre-cultures in anaerobic shaken bottles and for batch processes in the 1L stirred-tank bioreactor with *C. carboxidivorans* and *C. autoethanogenum*; Table S2: Total gas uptake of CO, CO_2, and H_2, carbon in products, biomass, and medium, and carbon balance recovery of the reference batch processes with *C. carboxidivorans* in three individual reference batch processes, in processes with real syngas from gasification of biomass without redox control, and with redox control by supply of cysteine hydrochloride solution; Table S3: Total gas uptake of CO, CO_2, and H_2, carbon in products, biomass, and medium, and carbon balance recovery of the reference batch processes with *C. carboxidivorans* in three individual reference batch processes and in two processes with real syngas from gasification of biomass with oxygen reduction in a tube reactor with Actisorb O3 as Pd catalyst; Table S4: Total gas uptake of CO, CO_2, and H_2, carbon in products, biomass, and medium, and carbon balance recovery of the reference batch processes with *C. autoethanogenum* in three individual reference batch processes, and in one process with real syngas from gasification of biomass with oxygen reduction in a tube reactor with Actisorb O3 as Pd catalyst; Figure S1: Comparison of redox potential of syngas fermentation batch processes with *C. carboxidivorans* (**A**,**C**,**E**) and *C. autoethanogenum* (**B**,**D**) in reference batch processes (**A**,**B**), using biogenic syngas with oxygen reduction (**C**,**D**), and without oxygen reduction (**E**) without regulation of redox potential (E black line) and with controlled redox potential to < −250mV by 40 g L^{-1} cysteine hydrochloride solution (E light grey line). Reaction conditions were constant at T = 37 °C, P V^{-1} = 15.1 W L^{-1}, F_{gas} = 5 NL h^{-1}, pH = 6.0 (uncontrolled for *C. carboxidivorans*), p_{CO} = 300 mbar, p_{H2} = 220 mbar, p_{CO2} = 90 mbar, p_{N2} = 390 mbar; Figure S2: Comparison of gas consumption of CO (black line), CO_2 (dark grey dashed line), and H_2 (light grey dashed line) for three autotrophic reference batch processes using *C. carboxidivorans* with artificial syngas (**A**–**F**) having two batch processes with real syngas from entrained flow gasification of biogenic residues (torrefied wood, TorrCoal) without regulation of redox potential (**G** and **H**) and with controlled redox potential to < −250 mV by 40 g L^{-1} cysteine hydrochloride solution (**I** and **J**). Reaction conditions were constant at T = 37 C, P V^{-1} = 15.1 W L^{-1}, F_{gas} = 5 NL h^{-1}, $pH_{initial}$ = 6.0 (uncontrolled unless > pH 6.4), p_{CO} = 300 mbar, p_{H2} = 220 mbar, p_{CO2} = 90 mbar, p_{N2} = 390 mbar; Figure S3: Comparison of gas consumption of CO (black line), CO_2 (dark grey dashed line), and H_2 (light grey dashed line) for three autotrophic reference batch processes using *C. carboxidivorans* with artificial syngas (**A**–**F**) having two batch processes with real syngas from entrained flow gasification of biogenic residues (torrefied wood, TorrCoal) with reduction of oxygen by a plug flow reactor (inner diameter 10 mm; length 1000 mm) with 30 g Actisorb O3 and 10 g silica beads at a temperature of 50 °C (**G**–**J**). Reaction conditions were constant at T = 37 °C, P V^{-1} = 15.1 W L^{-1}, F_{gas} = 5 NL h^{-1}, $pH_{initial}$ = 6.0 (uncontrolled unless > pH 6.4), p_{CO} = 300 mbar, p_{H2} = 220 mbar, p_{CO2} = 90 mbar, p_{N2} = 390 mbar and Figure S4: Comparison of gas consumption of CO (black line), CO_2 (dark grey dashed line), and H_2 (light grey dashed line) of three autotrophic reference batch processes using *C. autoethanogenum* with artificial syngas (**A**–**F**) having one batch process with real syngas from entrained flow gasification of biogenic residues (torrefied wood, TorrCoal) with reduction of oxygen by a plug flow reactor (inner diameter 10 mm; length 1000 mm) with 30 g Actisorb O3 and 10 g silica beads at a temperature of 50 °C (**G**–**H**). Reaction conditions were constant at T = 37 °C, P V^{-1} = 15.1 W L^{-1}, F_{gas} = 5 NL h^{-1}, pH = 6.0 (controlled with 3 M NaOH), p_{CO} = 300 mbar, p_{H2} = 220 mbar, p_{CO2} = 90 mbar, p_{N2} = 390 mbar.

Author Contributions: Conceptualization, A.R. and D.W.-B.; methodology, A.R. and A.O. (syngas fermentation), P.L., P.J. and S.F. (gasification); formal analysis, A.R.; investigation, A.R. and A.O.; data curation, A.R. and D.W.-B.; writing—original draft preparation, A.R. (syngas fermentation), and P.L. (gasification); writing—review and editing, D.W.-B.; visualization, A.R.; supervision, project administration, D.W.-B. (syngas fermentation), S.F. (gasification); funding acquisition, S.F. and D.W.-B.; All authors have read and agreed to the published version of the manuscript.

Funding: This research was funded by the Federal Ministry of Education and Research (BMBF), Germany (ReGasFerm—Grant number 031B0677A).

Institutional Review Board Statement: Not applicable.

Informed Consent Statement: Not applicable.

Data Availability Statement: The original contributions presented in the study are included in the article/Supplementary Material; further inquiries can be directed to the corresponding author/s.

Acknowledgments: The authors gratefully thank Luis Oliveira (Institute of Biochemical Engineering, Technical University of Munich), and Hartmut Spliethoff (Institute of Energy Systems, Technical University of Munich) for their ongoing support and many helpful discussions. The support of Anton Rückel, Anne Oppelt, Philipp Leuter, and Philipp Johne from the TUM Graduate School (Technical University of Munich, Germany) is acknowledged as well.

Conflicts of Interest: The authors declare no conflict of interest. The funders had no role in the design of the study; in the collection, analyses, or interpretation of data; in the writing of the manuscript; or in the decision to publish the results.

References

1. Kremling, M.; Briesemeister, L.; Gaderer, M.; Fendt, S.; Spliethoff, H. Oxygen-blown entrained flow gasification of biomass: Impact of fuel parameters and oxygen stoichiometric ratio. *Energy Fuels* **2017**, *31*, 3949–3959. [CrossRef]
2. Kremling, M.B. Experimentelle Untersuchungen zur Sauerstoffgeblasenen Flugstromvergasung von Staubförmiger Biomasse. Ph.D. Thesis, Technical University of Munich, Verlag Dr. Hut. Munich, Germany, 2018.
3. Xu, D.; Tree, D.R.; Lewis, R.S. The effects of syngas impurities on syngas fermentation to liquid fuels. *Biomass Bioenergy* **2011**, *35*, 2690–2696. [CrossRef]
4. Infantes, A.; Kugel, M.; Raffelt, K.; Neumann, A. Side-by-side Comparison of clean and biomass-derived, impurity-containing syngas as substrate for acetogenic fermentation with *Clostridium ljungdahlii*. *Fermentation* **2020**, *6*, 84. [CrossRef]
5. Ahmed, A.; Cateni, B.G.; Huhnke, R.L.; Lewis, R.S. Effects of biomass-generated producer gas constituents on cell growth, product distribution and hydrogenase activity of *Clostridium carboxidivorans* P7T. *Biomass Bioenergy* **2006**, *30*, 665–672. [CrossRef]
6. Liakakou, E.T.; Infantes, A.; Neumann, A.; Vreugdenhil, B.J. Connecting gasification with syngas fermentation: Comparison of the performance of lignin and beech wood. *Fuel* **2021**, *290*, 120054. [CrossRef]
7. Benevenuti, C.; Amaral, P.; Ferreira, T.; Seidl, P. Impacts of syngas composition on anaerobic fermentation. *Reactions* **2021**, *2*, 391–407. [CrossRef]
8. Broer, K.M.; Brown, R.C. Effect of equivalence ratio on partitioning of nitrogen during biomass gasification. *Energy Fuels* **2016**, *30*, 407–413. [CrossRef]
9. Schneider, J.; Grube, C.; Herrmann, A.; Rönsch, S. Atmospheric entrained-flow gasification of biomass and lignite for decentralized applications. *Fuel Process. Technol.* **2016**, *152*, 72–82. [CrossRef]
10. Briesemeister, L.; Kremling, M.; Fendt, S.; Spliethoff, H. Air-blown entrained-flow gasification of biomass: Influence of operating conditions on tar generation. *Energy Fuels* **2017**, *31*, 10924–10932. [CrossRef]
11. Dürre, P. Biobutanol: An attractive biofuel. *Biotechnol. J.* **2007**, *2*, 1525–1534. [CrossRef]
12. Köpke, M.; Mihalcea, C.; Bromley, J.C.; Simpson, S.D. Fermentative production of ethanol from carbon monoxide. *Curr. Opin. Biotechnol.* **2011**, *22*, 320–325. [CrossRef] [PubMed]
13. Liew, F.E.; Nogle, R.; Abdalla, T.; Rasor, B.J.; Canter, C.; Jensen, R.O.; Wang, L.; Strutz, J.; Chirania, P.; de Tissera, S.; et al. Carbon-negative production of acetone and isopropanol by gas fermentation at industrial pilot scale. *Nat. Biotechnol.* **2022**, *40*, 335–344. [CrossRef] [PubMed]
14. Schuchmann, K.; Müller, V. Autotrophy at the thermodynamic limit of life: A model for energy conservation in acetogenic bacteria. *Nat. Rev. Microbiol.* **2014**, *12*, 809–821. [CrossRef] [PubMed]
15. Ragsdale, S.W.; Pierce, E. Acetogenesis and the Wood-Ljungdahl pathway of CO(2) fixation. *Biochim. Biophys. Acta* **2008**, *1784*, 1873–1898. [CrossRef] [PubMed]
16. Doll, K.; Rückel, A.; Kämpf, P.; Wende, M.; Weuster-Botz, D. Two stirred-tank bioreactors in series enable continuous production of alcohols from carbon monoxide with *Clostridium carboxidivorans*. *Bioprocess Biosyst. Eng.* **2018**, *41*, 1403–1416. [CrossRef]

17. Liou, J.S.-C.; Balkwill, D.L.; Drake, G.R.; Tanner, R.S. *Clostridium carboxidivorans* sp. nov., a solvent-producing *Clostridium* isolated from an agricultural settling lagoon, and reclassification of the acetogen *Clostridium scatologenes* strain SL1 as *Clostridium drakei* sp. nov. *Int. J. Syst. Evol. Microbiol.* **2005**, *55*, 2085–2091. [CrossRef]
18. Rückel, A.; Hannemann, J.; Maierhofer, C.; Fuchs, A.; Weuster-Botz, D. Studies on syngas fermentation with *Clostridium carboxidivorans* in stirred-tank reactors with defined gas impurities. *Front. Microbiol.* **2021**, *12*. [CrossRef]
19. Hurst, K.M.; Lewis, R.S. Carbon monoxide partial pressure effects on the metabolic process of syngas fermentation. *Biochem. Eng. J.* **2010**, *48*, 159–165. [CrossRef]
20. Abrini, J.; Naveau, H.; Nyns, E.-J. *Clostridium autoethanogenum*, sp. nov., an anaerobic bacterium that produces ethanol from carbon monoxide. *Arch. Microbiol.* **1994**, *161*, 345–351. [CrossRef]
21. Oliveira, L.; Rückel, A.; Nordgauer, L.; Schlumprecht, P.; Hutter, E.; Weuster-Botz, D. Comparison of syngas-fermenting *Clostridia* in stirred-tank bioreactors and the effects of syngas impurities. *Microorganisms* **2022**, *10*, 681. [CrossRef]
22. Köpke, M.; Mihalcea, C.; Liew, F.; Tizard, J.H.; Ali, M.S.; Conolly, J.J.; Al-Sinawi, B.; Simpson, S.D. 2,3-butanediol production by acetogenic bacteria, an alternative route to chemical synthesis, using industrial waste gas. *Appl. Environ. Microbiol.* **2011**, *77*, 5467–5475. [CrossRef] [PubMed]
23. Abubackar, H.N.; Veiga, M.C.; Kennes, C. Carbon monoxide fermentation to ethanol by *Clostridium autoethanogenum* in a bioreactor with no accumulation of acetic acid. *Bioresour. Technol.* **2015**, *186*, 122–127. [CrossRef]
24. Abubackar, H.N.; Veiga, M.C.; Kennes, C. Biological conversion of carbon monoxide: Rich syngas or waste gases to bioethanol. *Biofuels Bioprod. Bioref.* **2011**, *5*, 93–114. [CrossRef]
25. Li, N.; Yang, J.; Chai, C.; Yang, S.; Jiang, W.; Gu, Y. Complete genome sequence of *Clostridium carboxidivorans* P7(T), a syngas-fermenting bacterium capable of producing long-chain alcohols. *J. Biotechnol.* **2015**, *211*, 44–45. [CrossRef]
26. Humphreys, C.M.; McLean, S.; Schatschneider, S.; Millat, T.; Henstra, A.M.; Annan, F.J.; Breitkopf, R.; Pander, B.; Piatek, P.; Rowe, P.; et al. Whole genome sequence and manual annotation of *Clostridium autoethanogenum*, an industrially relevant bacterium. *BMC Genom.* **2015**, *16*, 1085. [CrossRef] [PubMed]
27. Bruant, G.; Lévesque, M.-J.; Peter, C.; Guiot, S.R.; Masson, L. Genomic analysis of carbon monoxide utilization and butanol production by *Clostridium carboxidivorans* strain P7. *PLoS ONE* **2010**, *5*, e13033. [CrossRef]
28. Fernández-Naveira, Á.; Veiga, M.C.; Kennes, C. H-B-E (hexanol-butanol-ethanol) fermentation for the production of higher alcohols from syngas/waste gas. *J. Chem. Technol. Biotechnol.* **2017**, *92*, 712–731. [CrossRef]
29. Ganigué, R.; Sánchez-Paredes, P.; Bañeras, L.; Colprim, J. Low fermentation pH is a trigger to alcohol production, but a killer to chain elongation. *Front. Microbiol.* **2016**, *7*, 702. [CrossRef]
30. Ramió-Pujol, S.; Ganigué, R.; Bañeras, L.; Colprim, J. How can alcohol production be improved in carboxydotrophic *Clostridia*? *Process Biochem.* **2015**, *50*, 1047–1055. [CrossRef]
31. Ukpong, M.N.; Atiyeh, H.K.; de Lorme, M.J.M.; Liu, K.; Zhu, X.; Tanner, R.S.; Wilkins, M.R.; Stevenson, B.S. Physiological response of *Clostridium carboxidivorans* during conversion of synthesis gas to solvents in a gas-fed bioreactor. *Biotechnol. Bioeng.* **2012**, *109*, 2720–2728. [CrossRef]
32. Liew, F.; Henstra, A.M.; Köpke, M.; Winzer, K.; Simpson, S.D.; Minton, N.P. Metabolic engineering of *Clostridium autoethanogenum* for selective alcohol production. *Metab. Eng.* **2017**, *40*, 104–114. [CrossRef] [PubMed]
33. Cheng, C.; Bao, T.; Yang, S.-T. Engineering *Clostridium* for improved solvent production: Recent progress and perspective. *Appl. Microbiol. Biotechnol.* **2019**, *103*, 5549–5566. [CrossRef]
34. Haynes, W.M.; Lide, D.R.; Bruno, T.J. *CRC Handbook of Chemistry and Physics*; CRC Press: Boca Raton, FL, USA, 2016; ISBN 9781315380476.
35. Xu, D.; Lewis, R.S. Syngas fermentation to biofuels: Effects of ammonia impurity in raw syngas on hydrogenase activity. *Biomass Bioenergy* **2012**, *45*, 303–310. [CrossRef]
36. Datar, R.P.; Shenkman, R.M.; Cateni, B.G.; Huhnke, R.L.; Lewis, R.S. Fermentation of biomass-generated producer gas to ethanol. *Biotechnol. Bioeng.* **2004**, *86*, 587–594. [CrossRef] [PubMed]
37. Itoh, H.; Hirota, A.; Hirayama, K.; Shin, T.; Murao, S. Properties of Ascorbate Oxidase Produced by *Acremonium* sp. HI-25. *Biosci. Biotechnol. Biochem.* **1995**, *59*, 1052–1056. [CrossRef]
38. Picton, R.; Eggo, M.C.; Merrill, G.A.; Langman, M.J.S.; Singh, S. Mucosal protection against sulphide: Importance of the enzyme rhodanese. *Gut* **2002**, *50*, 201–205. [CrossRef] [PubMed]
39. Allais, J.J.; Louktibi, A.; Baratti, J. Oxidation of Methanol by the Yeast *Pichia pastoris*. Purification and Properties of the Formate Dehydrogenase. *Agric. Biol. Chem.* **1983**, *47*, 2547–2554. [CrossRef]
40. Meakin, G.E.; Jepson, B.J.N.; Richardson, D.J.; Bedmar, E.J.; Delgado, M.J. The role of *Bradyrhizobium japonicum* nitric oxide reductase in nitric oxide detoxification in soya bean root nodules. *Biochem. Soc. Trans.* **2006**, *34*, 195–196. [CrossRef]
41. Emerson, D.F.; Woolston, B.M.; Liu, N.; Donnelly, M.; Currie, D.H.; Stephanopoulos, G. Enhancing hydrogen-dependent growth of and carbon dioxide fixation by *Clostridium ljungdahlii* through nitrate supplementation. *Biotechnol. Bioeng.* **2019**, *116*, 294–306. [CrossRef]
42. Fröstl, J.M.; Seifritz, C.; Drake, H.L. Effect of nitrate on the autotrophic metabolism of the acetogens *Clostridium thermoautotrophicum* and *Clostridium thermoaceticum*. *J. Bacteriol.* **1996**, *178*, 4597–4603. [CrossRef]
43. Seifritz, C.; Drake, H.L.; Daniel, S.L. Nitrite as an energy-conserving electron sink for the acetogenic bacterium *Moorella thermoacetica*. *Curr. Microbiol.* **2003**, *46*, 329–333. [CrossRef] [PubMed]

44. Oswald, F.; Zwick, M.; Omar, O.; Hotz, E.N.; Neumann, A. Growth and Product Formation of *Clostridium ljungdahlii* in Presence of Cyanide. *Front. Microbiol.* **2018**, *9*, 1213. [CrossRef] [PubMed]
45. Hyman, M.R.; Ensign, S.A.; Arp, D.J.; Ludden, P.W. Carbonyl sulfide inhibition of CO dehydrogenase from *Rhodospirillum rubrum*. *Biochemistry* **1989**, *28*, 6821–6826. [CrossRef] [PubMed]
46. Müller, V.; Aufurth, S.; Rahlfs, S. The Na+ cycle in *Acetobacterium woodii*: Identification and characterization of a Na+ translocating F1F0-ATPase with a mixed oligomer of 8 and 16 kDa proteolipids. *Biochim. Biophys. Acta (BBA) Bioenerg.* **2001**, *1505*, 108–120. [CrossRef]
47. Maden, B.E.H. Tetrahydrofolate and tetrahydromethanopterin compared: Functionally distinct carriers in C1 metabolism. *Biochem. J.* **2000**, *350*, 609–629. [CrossRef]
48. Vanoni, M.A.; Matthews, R.G. Kinetic isotope effects on the oxidation of reduced nicotinamide adenine dinucleotide phosphate by the flavoprotein methylenetetrahydrofolate reductase. *Biochemistry* **1984**, *23*, 5272–5279. [CrossRef]
49. Liu, C.-G.; Xue, C.; Lin, Y.-H.; Bai, F.-W. Redox potential control and applications in microaerobic and anaerobic fermentations. *Biotechnol. Adv.* **2013**, *31*, 257–265. [CrossRef]
50. Karnholz, A.; Küsel, K.; Gössner, A.; Schramm, A.; Drake, H.L. Tolerance and metabolic response of acetogenic bacteria toward oxygen. *Appl. Environ. Microbiol.* **2002**, *68*, 1005–1009. [CrossRef]
51. Kundiyana, D.K.; Huhnke, R.L.; Wilkins, M.R. Syngas fermentation in a 100-L pilot scale fermentor: Design and process considerations. *J. Biosci. Bioeng.* **2010**, *109*, 492–498. [CrossRef]
52. Groher, A.; Weuster-Botz, D. Comparative reaction engineering analysis of different acetogenic bacteria for gas fermentation. *J. Biotechnol.* **2016**, *228*, 82–94. [CrossRef]
53. Daniell, J.; Köpke, M.; Simpson, S. Commercial biomass syngas fermentation. *Energies* **2012**, *5*, 5372–5417. [CrossRef]
54. Battino, R.; Seybold, P.G.; Campanell, F.C. Correlations involving the solubility of gases in water at 298.15 K and 101325 Pa. *J. Chem. Eng. Data* **2011**, *56*, 727–732. [CrossRef]
55. Liew, F.; Kopke, M.; Dennis, S. Gas fermentation for commercial biofuels production. In *Liquid, Gaseous and Solid Biofuels—Conversion Techniques*; Fang, Z., Ed.; InTech: Houston, TX, USA, 2013; ISBN 978-953-51-1050-757.
56. Liu, X.; Fabos, V.; Taylor, S.; Knight, D.W.; Whiston, K.; Hutchings, G.J. One-Step Production of 1,3-Butadiene from 2,3-Butanediol Dehydration. *Chemistry* **2016**, *22*, 12290–12294. [CrossRef] [PubMed]
57. Ezeji, T.C.; Qureshi, N.; Blaschek, H.P. Butanol fermentation research: Upstream and downstream manipulations. *Chem. Rec.* **2004**, *4*, 305–314. [CrossRef] [PubMed]
58. Hu, P.; Bowen, S.H.; Lewis, R.S. A thermodynamic analysis of electron production during syngas fermentation. *Bioresour. Technol.* **2011**, *102*, 8071–8076. [CrossRef] [PubMed]
59. Heffernan, J.K.; Valgepea, K.; de Souza Pinto Lemgruber, R.; Casini, I.; Plan, M.; Tappel, R.; Simpson, S.D.; Köpke, M.; Nielsen, L.K.; Marcellin, E. Enhancing CO_2-valorization using *Clostridium autoethanogenum* for sustainable fuel and chemicals production. *Front. Bioeng. Biotechnol.* **2020**, *8*, 204. [CrossRef]
60. Riegler, P.; Chrusciel, T.; Mayer, A.; Doll, K.; Weuster-Botz, D. Reversible retrofitting of a stirred-tank bioreactor for gas-lift operation to perform synthesis gas fermentation studies. *Biochem. Eng. J.* **2019**, *141*, 89–101. [CrossRef]
61. Weuster-Botz, D. Process Engineering Aspects for the Microbial Conversion of C1 Gases. *Adv. Biochem. Eng. Biotechnol.* **2022**, *180*, 33–56. [CrossRef]
62. Youssef, A.A. Fluid Dynamics and Scale-Up of Bubble Columns with Internals. Ph.D. Thesis, Washington University in St. Louis, St. Louis, MO, USA, 2010. All Theses and Dissertations (ETDs). [CrossRef]
63. Hernández, J.J.; Aranda, G.; Barba, J.; Mendoza, J.M. Effect of steam content in the air–steam flow on biomass entrained flow gasification. *Fuel Processing Technology* **2012**, *99*, 43–55. [CrossRef]
64. Vishwajeet; Pawlak-Kruczek, H.; Baranowski, M.; Czerep, M.; Chorążyczewski, A.; Krochmalny, K.; Ostrycharczyk, M.; Ziółkowski, P.; Madejski, P.; Mączka, T.; et al. Entrained flow plasma gasification of sewage sludge–Proof-of-concept and fate of inorganics. *Energies* **2022**, *15*, 1948. [CrossRef]
65. Mazzoni, L.; Janajreh, I.; Elagroudy, S.; Ghenai, C. Modeling of plasma and entrained flow co-gasification of MSW and petroleum sludge. *Energy* **2020**, *196*, 117001. [CrossRef]
66. Agon, N.; Hrabovský, M.; Chumak, O.; Hlína, M.; Kopecký, V.; Masláni, A.; Bosmans, A.; Helsen, L.; Skoblja, S.; van Oost, G.; et al. Plasma gasification of refuse derived fuel in a single-stage system using different gasifying agents. *Waste Manag.* **2016**, *47*, 246–255. [CrossRef] [PubMed]
67. Kobayashi, J.; Kawamoto, K.; Fukushima, R.; Tanaka, S. Woody biomass and RPF gasification using reforming catalyst and calcium oxide. *Chemosphere* **2011**, *83*, 1273–1278. [CrossRef] [PubMed]